Liquid–Liquid Equilibria for Copolymer Mixtures from a Perturbed Hard-Sphere-Chain Equation of State

Toshiaki Hino, Yuhua Song, and John M. Prausnitz*

Department of Chemical Engineering, University of California, Berkeley, and Chemical Sciences Division, Lawrence Berkeley Laboratory, Berkeley, California 94720

Received March 29, 1994; Revised Manuscript Received July 5, 1994®

ABSTRACT: A perturbed hard-sphere-chain (PHSC) equation of state for real copolymer mixtures is based on a modified form of Chiew's equation of state for athermal mixtures of heteronuclear hard-sphere chains. The PHSC equation of state includes a van der Waals perturbation whose parameters are related to the intermolecular potential as suggested by Song and Mason. In the present model, sequence distribution in a polymer is introduced only into the hard-sphere-chain reference state; attractive forces are averaged, independent of sequence distribution. Theoretical coexistence curves and miscibility maps were computed for binary random copolymer mixtures containing two or three kinds of segments. The PHSC equation of state can predict simultaneous occurrence of a lower critical solution temperature and an upper critical solution temperature in the temperature–composition phase diagram of high-molecular-weight copolymer blends. Theoretical and experimental coexistence curves and miscibility maps show good agreement for systems containing two kinds of segments.

Introduction

Equation-of-state theories are useful for describing the phase equilibria of solutions and blends containing copolymers. A brief review of equations of state for copolymer systems is given by Wohlfarth.[1] Equations of state based on free-volume or lattice–fluid models[1] have an advantage over incompressible lattice theories[2] because they can predict a lower critical solution temperature (LCST) at elevated temperature as well as an upper critical solution temperature (USCT). LCST behavior is a common phenomenon in polymer blends including those that contain copolymers. In addition, an equation of state is also able to describe the effect of pressure on phase behavior.

An equation of state applicable to polymer systems is the perturbed hard-sphere-chain (PHSC) equation recently developed by Song *et al.*[3–6] These authors[3] first presented a hard-sphere-chain (HSC) equation of state for athermal homonuclear and heteronuclear HSC mixtures by generalizing Chiew's equation of state for mixtures of hard-sphere chains[7] through the Carnahan–Starling radial distribution function for hard-sphere mixtures at contact. Compared to Chiew's original equation of state, the new equation of state for athermal systems was expressed more succinctly. For real polymer fluids, Song *et al.*[4–6] introduced a van der Waals perturbation and the Song–Mason method[4,8] to relate equation-of-state parameters to the intermolecular potential. The Song–Mason method is used to scale the effective van der Waals covolume, b (i.e., second virial coefficient of hard spheres), and the attractive energy parameter, a, in terms of the well depth of the pair potential, ϵ, and the distance of separation at minimum potential energy, σ. In this method, the temperature dependences of parameters a and b are given by two known universal functions of a reduced temperature.

For a homopolymer, the PHSC equation of state requires three parameters: number of effective hard spheres per molecule, r; segmental diameter, σ; and nonbonded segment pair interaction energy, ϵ. These parameters were regressed from available volumetric and vapor-pressure data for a variety of normal fluids and several homopolymers; they are tabulated in ref 4. For a homopolymer, one of the regressed characteristic quantities is r/M, where M is the molecular weight of the polymer. The PHSC equation of state was shown to fit the homopolymer pressure–volume–temperature data much better than the lattice–fluid equation of state[9,10] and slightly better than the statistical association fluid theory (SAFT)[11,12] equation of state; lattice–fluid and SAFT equations of state also require three molecular parameters to describe the properties of pure fluids including homopolymers. In addition, the PHSC equation of state fits the properties of normal fluids better than the SAFT equation of state and essentially as well as the lattice–fluid equation of state.[4]

For mixtures, no mixing rules are required for the hard-sphere-chain contribution. For the perturbation term, a standard one-fluid theory was used.[5,6] For several binary mixtures including homopolymer solutions and homopolymer/homopolymer blends,[6] calculated liquid–liquid coexistence curves are in good agreement with experiment.

In this paper we present an extension of the PHSC equation of state for copolymer mixtures. Theoretical coexistence curves and miscibility maps are computed for binary random copolymer mixtures containing two and three kinds of segments. These mixtures are denoted as $(A_XB_{1-X})_{r_1}/(A_YB_{1-Y})_{r_2}$ and $(A_XB_{1-X})_{r_1}/C_YB_{1-Y})_{r_2}$, where r_i is the number of hard spheres per molecule of component i and X and Y are segment number fractions for segments A, A, and C in components 1 and 2, respectively.

Theoretical coexistence curves and miscibility maps are compared with experiment for mixtures of type $(A_XB_{1-X})_{r_1}/(A_YB_{1-Y})_{r_2}$ containing poly(styrene-*co*-butadiene), poly(butyl methacrylate-*co*-methyl methacrylate), and poly(styrene-*co*-butyl methacrylate) random copolymers.

Theory

Equation of State for Pure Copolymers. Using the modified Chiew equation of state as the reference state,[3] the PHSC equation of state for pure heteronuclear polymer molecules consisting of r effective hard spheres is

* To whom correspondence should be addressed.
® Abstract published in *Advance ACS Abstracts,* August 15, 1994.

0024-9297/94/2227-5681$04.50/0

$$\frac{p}{\rho k_B T} = 1 + \rho \sum_{k=1}^{r}\sum_{l=1}^{r} b_{kl} g_{kl} - \sum_{k=1}^{r-1}[g_{k,k+1} - 1] - \frac{\rho}{k_B T}\sum_{k=1}^{r}\sum_{l=1}^{r} a_{kl} \quad (1)$$

where p is the pressure, $\rho = N/V$ (N is the number of molecules and V is the volume) is the number density, k_B is the Boltzmann constant, T is the absolute temperature, and subscripts k and l denote the kth and lth segments, respectively, of hard-sphere chains. Equation 1 obeys the ideal-gas limit as $\rho \to 0$. In eq 1 a_{kl} is a parameter which reflects the strength of attractive forces between two effective hard spheres, b_{kl} represents the second virial coefficient of hard spheres or the van der Waals covolume for effective hard spheres that accounts for the excluded volume due to the repulsive forces only in the Song–Mason theory,[8] and g_{kl} is the pair radial distribution function of hard spheres when kth and lth segments are at contact. These parameters and the pair distribution function are temperature dependent, as shown later. Equation 1 is for hard-sphere chains consisting of an arbitrary number of chemically different segments. The segments in the chain need *not* have the same size.

We consider copolymers consisting of two types of segments A and B:

$$(A_X B_{1-X})_r \quad (2)$$

where X is the number fraction of segment of type A. In a polymer chain, the number of segments of type A per molecule is given by r_A and that of type B is given by r_B:

$$r_A = rX \quad (3)$$

$$r_B = r(1 - X) \quad (4)$$

For copolymers eq 1 reduces to

$$\frac{p}{\rho k_B T} = 1 + \rho(r_A r_A b_{AA} g_{AA} + r_A r_B b_{AB} g_{AB} + r_B r_A b_{BA} g_{BA} + r_B r_B b_{BB} g_{BB}) - (n_{AA}[g_{AA} - 1] + n_{AB}[g_{AB} - 1] + n_{BA}[g_{BA} - 1] + n_{BB}[g_{BB} - 1]) - \frac{\rho}{k_B T}(r_A r_A a_{AA} + r_A r_B a_{AB} + r_B r_A a_{BA} + r_B r_B a_{BB}) \quad (5)$$

where $n_{\alpha\beta}$ (α,β = A,B) is the number of α–β sequences (i.e., bonding pairs) per molecule in hard-sphere chains and

$$n_{AA} + n_{AB} + n_{BA} + n_{BB} = r - 1 \quad (6)$$

In the following equations, the type of segment–segment interaction is specified by subscripts α and β; these subscripts appear in parameters and pair distribution functions.

Parameters $a_{\alpha\beta}$ and $b_{\alpha\beta}$ and the radial distribution function, $g_{\alpha\beta}$, are given by

$$a_{\alpha\alpha} = \frac{2}{3}\pi\sigma_\alpha^3 \epsilon_\alpha F_a(\tilde{T}_\alpha) \quad (7)$$

$$a_{AB} = a_{BA} = \frac{2}{3}\pi\sigma_{AB}^3 \epsilon_{AB}[F_a(\tilde{T}_A)\, F_a(\tilde{T}_B)]^{1/2} \quad (8)$$

$$b_{\alpha\alpha} = b_\alpha = \frac{2}{3}\pi\sigma_\alpha^3 F_b(\tilde{T}_\alpha) \quad (9)$$

$$b_{AB} = b_{BA} = \frac{1}{8}(b_A^{1/3} + b_B^{1/3})^3 \quad (10)$$

$$g_{\alpha\beta} = g_{\beta\alpha} = \frac{1}{1-\eta} + \frac{3}{2}\frac{\xi_{\alpha\beta}}{(1-\eta)^2} + \frac{1}{2}\frac{\xi_{\alpha\beta}^2}{(1-\eta)^3} \quad (11)$$

where α and β (α,β = A,B) specify the type of segment and η is the packing fraction given by

$$\eta = \frac{\rho}{4}(r_A b_A + r_B b_B) \quad (12)$$

and

$$\xi_{\alpha\beta} = \xi_{\beta\alpha} = \frac{\rho}{4}\left(\frac{b_\alpha b_\beta}{b_{\alpha\beta}}\right)^{1/3}(r_A b_A^{2/3} + r_B b_B^{2/3}) \quad (13)$$

In eqs 7–9, σ_α (α = A,B) and σ_{AB} are the separation distances between similar and dissimilar segments, respectively, at the minimum potential energies ϵ_α (α = A,B) and ϵ_{AB}, respectively, in the segment–segment pair potential. Equation 10 assumes additivity of effective hard-sphere diameters of unlike segments. Equations 11 and 13 are the results of a generalization of the radial distribution function at contact from the Carnahan–Starling equation to copolymer systems; derivation of these equations is given by ref 3.

In equations 7–9, F_a and F_b are known universal functions in terms of reduced temperature defined as[4]

$$\tilde{T}_\alpha = \frac{k_B T}{\epsilon_\alpha s(r)} \quad (14)$$

where $s(r)$ is a scaling parameter. Equations 7 and 9 are the results of the Song–Mason method,[4,8] which scales the effective van der Waals covolume, b (i.e., the second virial coefficient of hard spheres), and the attractive energy parameter, a, in terms of the well depth of the pair potential, ϵ, and the distance of separation at minimum potential energy, σ. The universal functions F_a and F_b account for the temperature dependences of parameters a and b, respectively. Equation 8 assumes a geometric mean of F_a for a segment A and that for a segment B to calculate the temperature dependence of the attractive energy parameter between a pair of dissimilar segments A and B. The universal functions are obtained from volumetric and vapor-pressure data for argon and for methane as indicated previously.[4] They are represented accurately by the following empirical relations:[4,13]

$$F_a(\tilde{T}_\alpha) = 0.7170 + 1.9003 \exp(-0.5152\tilde{T}_\alpha) \quad (15)$$

$$F_b(\tilde{T}_\alpha) = 0.5849 \exp(-0.4772\tilde{T}_\alpha) + (1 - 0.5849)[1 - \exp(-1.0669\tilde{T}_\alpha^{-1/4})] \quad (16)$$

The scaling parameter $s(r)$ in the reduced temperature, eq 14, arises from the scaling of F_a and F_b from single-sphere systems to systems containing polymer molecules. This parameter was originally introduced for homonuclear hard-sphere chains (i.e., homopolymers)[4] consisting of r tangent spheres. Although copolymers can be made of hard spheres of different sizes and interaction energies, $s(r)$ for copolymers is assumed to be a unique function of the total number of hard spheres per molecule. The function $s(r)$ is given in ref 4.

The effect of sequence distribution is not incorporated into the perturbation term in eqs 1 and 5. In principle, the effect of sequence distribution can be introduced by

expanding the perturbation term by the fraction of particular sequences (e.g., dyads and triads) in place of segment fraction.[14] Such a method, however, requires additional interaction energy parameters. Finally, in this paper we use the following combining rules to obtain parameters σ_{AB} and ϵ_{AB} in eq 8:

$$\sigma_{AB} = 1/2(\sigma_A + \sigma_B) \tag{17}$$

$$\epsilon_{AB} = (\epsilon_A\epsilon_B)^{1/2}(1 - \kappa_{AB}) \tag{18}$$

where κ_{AB} is an adjustable intersegmental parameter.

Equation of State for Copolymer Mixtures. Equation 1 is readily extended to mixtures of heteronuclear polymer molecules. The PHSC equation of state for mixtures of heteronuclear polymer molecules is

$$\frac{p}{\rho k_B T} = 1 + \rho \sum_{i=1}^{m}\sum_{j=1}^{m} x_i x_j \left[\sum_{k=1}^{r_i}\sum_{l=1}^{r_j} b_{ij,kl} g_{ij,kl}\right] - \sum_{i=1}^{m} x_i \times \sum_{k=1}^{r_i-1}\left[g_{ii,k,k+1} - 1\right] - \frac{\rho}{k_B T}\sum_{i=1}^{m}\sum_{j=1}^{m} x_i x_j \left[\sum_{k=1}^{r_i}\sum_{l=1}^{r_j} a_{ij,kl}\right] \tag{19}$$

where m is the number of compponents and x_i is the mole fraction of component i. The number of effective hard spheres per molecule of component i is designated by r_i. In eq 19, subscripts k and l denote the kth and lth segments, respectively, of hard-sphere chains. The physical significances of parameters $a_{ij,kl}$ and $b_{ij,kl}$ and pair distribution function $g_{ij,kl}$ for mixtures are the same as those for pure fluids.

We consider first binary mixtures of copolymers consisting of two types of segments A and B:

$$(A_X B_{1-X})_{r_1}/(A_Y B_{1-Y})_{r_2} \tag{20}$$

The number of segments of type A, $r_{1,A}$, and that of B, $r_{1,B}$, of component 1 are given by r_1X and $r_1(1-X)$, respectively. For binary mixtures of copolymers, eq 19 is

$$\frac{p}{\rho k_B T} = 1 + \rho \sum_{i=1}^{2}\sum_{j=1}^{2} x_i x_j [r_{i,A} r_{j,A} b_{ij,AA} g_{ij,AA} + r_{i,A} r_{j,B} b_{ij,AB} g_{ij,AB} + r_{i,B} r_{j,A} b_{ij,BA} g_{ij,BA} + r_{i,B} r_{j,B} b_{ij,BB} g_{ij,BB}] - \sum_{i=1}^{2} x_i [n_{i,AA}(g_{ii,AA} - 1) + n_{i,AB}(g_{ii,AB} - 1) + n_{i,BA}(g_{ii,BA} - 1) + n_{i,BB}(g_{ii,BB} - 1)] - \frac{\rho}{k_B T}\sum_{i=1}^{2}\sum_{j=1}^{2} x_i x_j [r_{i,A} r_{j,A} a_{ij,AA} + r_{i,A} r_{j,B} a_{ij,AB} + r_{i,B} r_{j,A} a_{ij,BA} + r_{i,B} r_{j,B} a_{ij,BB}] \tag{21}$$

where $n_{i,\alpha\beta}$ (i = 1,2; α,β = A,B) is the number of α–β sequences per molecule in component i. With a substitution of appropriate segments into segments A and B, eq 21 is also applicable to mixtures of type $(A_X B_{1-X})_{r_1}/(C_Y B_{1-Y})_{r_2}$ and $(A_X B_{1-X})_{r_1}/(C_Y D_{1-Y})_{r_2}$. For mixtures of type $(A_X B_{1-X})_{r_1}/(C_Y B_{1-Y})_{r_2}$ we replace segment A of component 2 by segment C. Similarly, for mixtures of type $(A_X B_{1-X})_{r_1}/(C_Y D_{1-Y})_{r_2}$ we replace segments A and B of component 2 by segments C and D, respectively.

In this type of mixture, parameters $a_{ij,\alpha\beta}$ and $b_{ij,\alpha\beta}$ and the radial distribution function $g_{ij,\alpha\beta}$ are given by

$$a_{ii,\alpha\alpha} = \frac{2}{3}\pi\sigma_{i,\alpha}^{\ 3}\epsilon_{i,\alpha}F_a(\tilde{T}_{i,\alpha}) \tag{22}$$

$$a_{ij,\alpha\beta} = a_{ji,\beta\alpha} = \frac{2}{3}\pi\sigma_{ij,\alpha\beta}^{\ 3}\epsilon_{ij,\alpha\beta}[F_a(\tilde{T}_{i,\alpha})\,F_a(\tilde{T}_{j,\beta})]^{1/2} \tag{23}$$

$$b_{ii,\alpha\alpha} = b_{i,\alpha} = \frac{2}{3}\pi\sigma_{i,\alpha}^{\ 3}F_b(\tilde{T}_{i,\alpha}) \tag{24}$$

$$b_{ij,\alpha\beta} = b_{ji,\beta\alpha} = \frac{1}{8}(b_{i,\alpha}^{\ 1/3} + b_{j,\beta}^{\ 1/3})^3 \tag{25}$$

$$g_{ij,\alpha\beta} = g_{ji,\beta\alpha} = \frac{1}{1-\eta} + \frac{3}{2}\frac{\xi_{ij,\alpha\beta}}{(1-\eta)^2} + \frac{1}{2}\frac{\xi_{ij,\alpha\beta}^{\ 2}}{(1-\eta)^3} \tag{26}$$

where η is the packing fraction given by

$$\eta = \frac{\rho}{4}\sum_{i=1}^{2} x_i(r_{i,A} b_{i,A} + r_{i,B} b_{i,B}) \tag{27}$$

and

$$\xi_{ij,\alpha\beta} = \xi_{ji,\beta\alpha} = \frac{\rho}{4}\left[\frac{b_{i,\alpha}b_{j,\beta}}{b_{ij,\alpha\beta}}\right]^{1/3}\sum_{i=1}^{2} x_i(r_{i,A} b_{i,A}^{\ 2/3} + r_{i,B} b_{i,B}^{\ 2/3}) \tag{28}$$

$$\tilde{T}_{i,\alpha} = \frac{k_B T}{\epsilon_{i,\alpha} s(r_i)} \tag{29}$$

In eqs 22–29, subscripts i and j (i,j = 1,2) and α and β (α,β = A,B) specify the component and type of segment, respectively. The universal functions F_a and F_b in eqs 22–24 are given by eqs 15 and 16, respectively. The scaling parameter, $s(r_i)$, in eq 29 is assumed to be a unique function of the total number of hard spheres of component i per molecule.

We use combining rules similar to eqs 17 and 18 to define $\sigma_{ij,\alpha\beta}$ and $\epsilon_{ij,\alpha\beta}$, respectively:

$$\sigma_{ij,\alpha\beta} = \sigma_{ji,\beta\alpha} = 1/2(\sigma_{i,\alpha} + \sigma_{j,\beta}) \tag{30}$$

$$\epsilon_{ij,\alpha\beta} = \epsilon_{ji,\beta\alpha} = (\epsilon_{i,\alpha}\epsilon_{j,\beta})^{1/2}(1 - \kappa_{ij,\alpha\beta}) \tag{31}$$

where $\kappa_{ij,\alpha\beta}$ is an adjustable intersegmental parameter whenever $\alpha \neq \beta$ and

$$\sigma_{ii,\alpha\alpha} = \sigma_{i,\alpha} \tag{32}$$

$$\epsilon_{ii,\alpha\alpha} = \epsilon_{i,\alpha} \tag{33}$$

Critical Condition and Coexistence Curve. The critical points and coexistence curves of mixtures can be found from the Helmholtz energy of the mixture, $A(T,x_i,\rho)$, which should not be confused with segment type A. The Helmholtz energy of the mixture is calculated from eq 19; it is[15]

$$\frac{A}{Nk_B T} = \sum_{i=1}^{m} x_i \frac{A_i^\circ}{Nk_B T} + \int_0^\rho \left(\frac{p}{\rho k_B T} - 1\right)\frac{d\rho}{\rho} + \sum_{i=1}^{m} x_i \ln\left(x_i \rho k_B T\right) = \sum_{i=1}^{m} x_i \frac{A_i^\circ}{Nk_B T} + \rho\sum_{i=1}^{m}\sum_{j=1}^{m} x_i x_j \times \left[\sum_{k=1}^{r_i}\sum_{l=1}^{r_j} b_{ij,kl} W_{ij,kl}\right] - \sum_{i=1}^{m} x_i \sum_{k=1}^{r_i-1} Q_{ii,k,k+1} - \frac{\rho}{k_B T}\sum_{i=1}^{m}\sum_{j=1}^{m} x_i x_j \left[\sum_{k=1}^{r_i}\sum_{l=1}^{r_j} a_{ij,kl}\right] + \sum_{i=1}^{m} x_i \ln\left(x_i \rho k_B T\right) \tag{34}$$

where A_i° is the Helmholtz energy of component i in the

reference state and

$$W_{ij,kl} = \frac{1}{\rho}\int_0^\rho g_{ij,kl}\, d\rho \tag{35}$$

$$Q_{ii,k,k+1} = \int_0^\rho [g_{ii,k,k+1} - 1]\frac{d\rho}{\rho} \tag{36}$$

The reference state is taken to be the pure ideal gas at unit pressure and at the temperature of the mixture containing the same number of molecules as the total number of molecules in the mixture.

For binary mixtures, the critical conditions are given by

$$\rho^2\left(\frac{\partial^2 A}{\partial x^2}\right)_{T,\rho}\left(\frac{\partial p}{\partial \rho}\right)_{T,x} - \left(\frac{\partial p}{\partial x}\right)_{T,\rho}^2 = 0 \tag{37}$$

$$\rho^3\left(\frac{\partial^3 A}{\partial x^3}\right)_{T,\rho}\left(\frac{\partial p}{\partial \rho}\right)_{T,x}^3 - 3\rho\left(\frac{\partial p}{\partial x}\right)_{T,\rho}\left(\frac{\partial^2 p}{\partial x^2}\right)_{T,\rho}\left(\frac{\partial p}{\partial \rho}\right)_{T,x}^2 + 3\rho\left(\frac{\partial p}{\partial x}\right)_{T,\rho}^2\left(\frac{\partial^2 p}{\partial x\,\partial \rho}\right)_T\left(\frac{\partial p}{\partial \rho}\right)_{T,x} - \left[2\left(\frac{\partial p}{\partial \rho}\right)_{T,x} + \rho\left(\frac{\partial^2 p}{\partial \rho^2}\right)_{T,x}\right]\left(\frac{\partial p}{\partial x}\right)_{T,\rho}^3 = 0 \tag{38}$$

where x is the mole fraction of component 1 or 2.

The chemical potential per molecule of component i, μ_i, is found from eq 34:

$$\mu_i = \left(\frac{\partial A}{\partial N_i}\right)_{T,\rho,N_{j\neq i}} \tag{39}$$

where N_i is the number of molecules of component i. The expression for the chemical potential is given in Appendix I. For a fixed temperature, the coexistence curve is calculated by equating the pressure and chemical potentials of coexisting phases:

$$p'(T,x',\rho') = p''(T,x'',\rho'') \tag{40}$$

$$\mu_1'(T,x',\rho') = \mu_1''(T,x'',\rho'') \tag{41}$$

$$\mu_2'(T,x',\rho') = \mu_2''(T,x'',\rho'') \tag{42}$$

where superscript primes denote the coexisting phases.

Results and Discussion

In this paper all the theoretical calculations were performed for liquids at zero pressure, an excellent approximation when the systems of interest are in the liquid state near atmospheric pressure.

Theoretical Coexistence Curves and Miscibility Maps. We first consider mixtures of random copolymers of type $(A_XB_{1-X})_{r_1}/(A_YB_{1-Y})_{r_2}$ containing two kinds of segments. For these systems the characteristic parameters in eqs 30–33 are

$$\sigma_{i,A} = \sigma_A, \quad \sigma_{i,B} = \sigma_B, \quad \epsilon_{i,A} = \epsilon_A, \quad \epsilon_{i,B} = \epsilon_B$$

$$\epsilon_{ij,AB} = \epsilon_{ij,BA} = \epsilon_{AB}, \quad \kappa_{ij,AB} = \kappa_{ij,BA} = \kappa_{AB} \quad (i,j = 1,2) \tag{43}$$

where

$$\epsilon_{AB} = (\epsilon_A\epsilon_B)^{1/2}(1 - \kappa_{AB}) \tag{44}$$

In addition, for truly random copolymers the number of k–l sequences (i.e., bonding pairs) of component 1, $n_{1,\alpha\beta}$ (α,β = A,B), may be calculated from a statistical average as

$$n_{1,AA} = X^2(r_1 - 1), \quad n_{1,AB} = n_{1,BA} = X(1 - X)(r_1 - 1), \quad n_{1,BB} = (1 - X)^2(r_1 - 1) \tag{45}$$

Similar expressions for $n_{2,\alpha\beta}$ are obtained by replacing X and subscript 1 by Y and 2, respectively, in the above equation. Here we consider only mixtures of random copolymers.

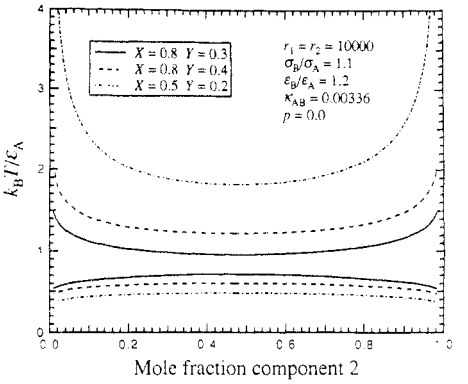

Figure 1. Theoretical coexistence curves for mixtures of random copolymers of type $(A_XB_{1-X})_{r_1}/(A_YB_{1-Y})_{r_2}$ with different copolymer compositions: $r_1 = r_2 = 10000$, $\sigma_B/\sigma_A = 1.1$, $\epsilon_B/\epsilon_A = 1.2$, $\kappa_{AB} = 0.00336$, $p = 0.0$.

Figure 1 shows theoretical coexistence curves for mixtures of random copolymers of type $(A_XB_{1-X})_{r_1}/(A_YB_{1-Y})_{r_2}$ ($r_1 = r_2 = 10000$) with different copolymer compositions X and Y. Since the total number of hard spheres per molecule is the same for both components, the only difference between components 1 and 2 is the copolymer composition. In this system, the miscibility of the mixture is expected to be enhanced as the difference in the copolymer compositions, $|X - Y|$, decreases. When $X = Y$, there is complete miscibility because, in that event, components 1 and 2 are identical.

The PHSC equation of state can produce both a lower critical solution temperature (LCST) and an upper critical solution temperature (UCST) in the temperature–composition phase diagram of high-molecular-weight copolymer blends. Figure 1 shows that the miscible temperature range (i.e., temperatures between LCST and UCST) increases as the difference in copolymer compositions declines.

UCSTs in Figure 1 result from a competition between energetic effects which are unfavorable and from entropy of mixing effects which favor miscibility. Since parameters are chosen such that the interactions between two copolymers of type $(A_XB_{1-X})_r$ differing in copolymer compositions are unfavorable, the mixtures in Figure 1 exhibit phase separations at low temperatures where energetic effects are dominant. LCSTs at elevated temperatures in Figure 1 are caused by the differences in compressibilities of components in the mixtures. In equation-of-state theories, compressibility disparities are related to differences in molecular sizes and in characteristic parameters of components.[16] For copolymers of type $(A_XB_{1-X})_r$ with known characteristic parameters for segments A and B, compressibilities depend on the copolymer composition as well as on the total number of effective hard spheres per molecule; the mixtures of type $(A_XB_{1-X})_{r_1}(A_YB_{1-Y})_{r_2}$ in Figure 1, therefore, are capable of exhibiting LCST type phase behavior, although the molecular sizes of the two copolymers in each mixture are almost the same.

Figure 2 shows theoretical coexistence curves for

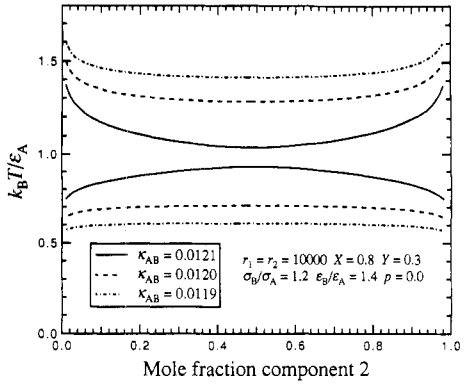

Figure 2. Theoretical coexistence curves for mixtures of random copolymers of type $(A_XB_{1-X})_{r_1}/(A_YB_{1-Y})_{r_2}$ ($r_1 = r_2 = 10000$, $X = 0.8$, $Y = 0.3$) with different values of intersegmental parameters κ_{AB}: $\sigma_B/\sigma_A = 1.2$, $\epsilon_B/\epsilon_A = 1.4$, $p = 0.0$.

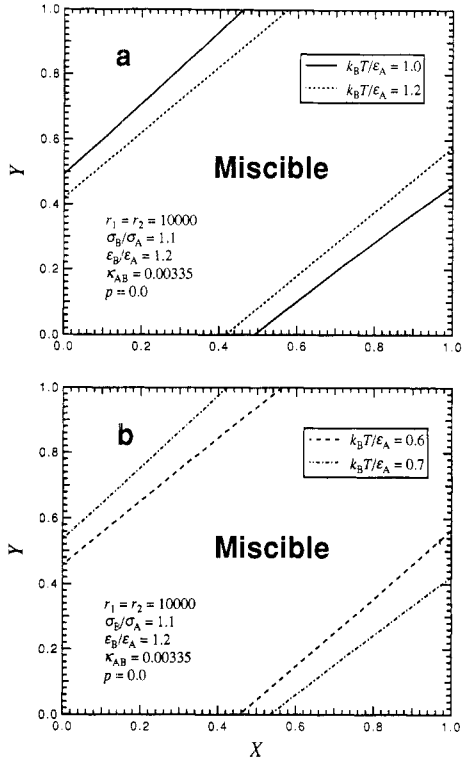

Figure 3. Miscibility maps of mixtures of random copolymers of type $(A_XB_{1-X})_{r_1}/(A_YB_{1-Y})_{r_2}$ at four reduced temperatures: $r_1 = r_2 = 10000$, $\sigma_B/\sigma_A = 1.1$, $\epsilon_B/\epsilon_A = 1.2$, $\kappa_{AB} = 0.00335$, $p = 0.0$. (a) Immiscibility due to LCST behavior; (b) immiscibility due to UCST behavior.

mixtures of random copolymers of type $(A_XB_{1-X})_{r_1}/(A_YB_{1-Y})_{r_2}$ ($r_1 = r_2 = 10000$, $X = 0.8$, $Y = 0.3$) with different values of intersegmental parameter κ_{AB}. Calculated coexistence curves are very sensitive to κ_{AB}. When the theory is applied to real systems, this parameter must be obtained by comparing the theoretical prediction with experiment.

Figure 3 shows miscibility maps of mixtures of random copolymers of type $(A_XB_{1-X})_{r_1}/(A_YB_{1-Y})_{r_2}$ at four reduced temperatures, $T_A = k_BT/\epsilon_A$. If a pair of X and Y are in the miscible region, a pair of copolymers with these compositions form a single homogeneous phase in all proportions. The phase diagram of the system shown in Figure 3 is similar to that shown in Figures 1 and 2, exhibiting both a LCST and an UCST. Therefore, the mixture of copolymers is completely miscible if the temperature of interest is between LCST and UCST. At temperatures in Figure 3a, immiscibility is caused by LCST

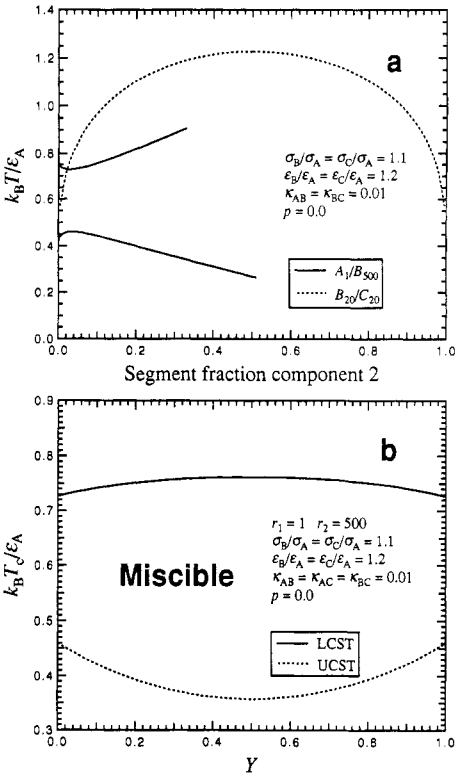

Figure 4. (a) Coexistence curves of two binary systems of type A_1/B_{500} and B_{20}/C_{20}: $\sigma_B/\sigma_A = \sigma_C/\sigma_A = 1.1$, $\epsilon_B/\epsilon_A = \epsilon_C/\epsilon_A = 1.2$, $\kappa_{AB} = \kappa_{BC} = 0.01$, $p = 0.0$. (b) Copolymer composition dependence of reduced LCST and UCST of copolymer solutions of type $A_1/(C_YB_{1-Y})_{500}$. System A_1/C_{500} is identical to system A_1/B_{500}.

behavior and the miscible area decreases as the temperature rises; however, at temperatures in Figure 3b, immiscibility is caused by UCST behavior and the miscible area increases as the temperature rises. The miscible area in Figure 3a decreases as the temperature rises because miscible pairs of copolymers in Figure 3a eventually become immiscible as the temperature rises above the LCST. Conversely, the miscible area in Figure 3b increases as the temperature rises because immiscible pairs of copolymers in Figure 3b eventually become miscible as the temperature exceeds the UCST.

Next, we consider mixtures of random copolymers of type $(A_XB_{1-X})_{r_1}/(C_YB_{1-Y})_{r_2}$ containing three kinds of segments. Equations 21–29 are applicable to the mixture of type $(A_XB_{1-X})_{r_1}/(C_YB_{1-Y})_{r_2}$ with the following substitutions of characteristic parameters for this system into those for the mixture of type $(A_XB_{1-X})_{r_1}/(A_YB_{1-Y})_{r_2}$:

$$\sigma_{1,A} = \sigma_A, \quad \sigma_{i,B} = \sigma_B, \quad \sigma_{2,A} = \sigma_C, \quad \epsilon_{1,A} = \epsilon_A, \quad \epsilon_{i,B} = \epsilon_{12,BB} = \epsilon_B, \quad \epsilon_{2,A} = \epsilon_C$$

$$\epsilon_{11,AB} = \epsilon_{12,AB} = \epsilon_{AB}, \quad \epsilon_{12,AA} = \epsilon_{AC}, \quad \epsilon_{12,BA} = \epsilon_{22,BA} = \epsilon_{BC}$$

$$\kappa_{11,AB} = \kappa_{12,AB} = \kappa_{AB}, \quad \kappa_{12,AA} = \kappa_{AC}, \quad \kappa_{12,BA} = \kappa_{22,BA} = \kappa_{BC} \quad (ij = 1,2) \quad (46)$$

where

$$\epsilon_{AB} = (\epsilon_A\epsilon_B)^{1/2}(1 - \kappa_{AB}), \quad \epsilon_{AC} = (\epsilon_A\epsilon_C)^{1/2}(1 - \kappa_{AC}), \quad \epsilon_{BC} = (\epsilon_B\epsilon_C)^{1/2}(1 - \kappa_{BC}) \quad (47)$$

An important system of this type is the mixture $A_{r_1}/(C_YB_{1-Y})_{r_2}$, which corresponds to copolymer–solvent solutions and to homopolymer/copolymer blends. In these systems the interesting question is how the miscibility of

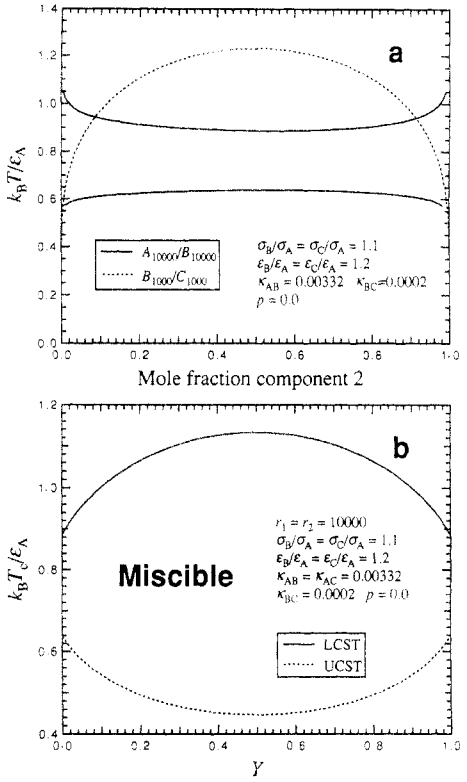

Figure 5. (a) Coexistence curves of two binary systems of type A_{10000}/B_{10000} and B_{1000}/C_{1000}: $\sigma_B/\sigma_A = \sigma_C/\sigma_A = 1.1$, $\epsilon_B/\epsilon_A = \epsilon_C/\epsilon_A = 1.2$, $\kappa_{AB} = 0.00332$, $\kappa_{BC} = 0.0002$, $p = 0.0$. (b) Copolymer composition dependence of reduced LCST and UCST of homopolymer/copolymer blends of type $A_{10000}/(C_YB_{1-Y})_{10000}$. System A_{10000}/C_{10000} is identical to system A_{10000}/B_{10000}.

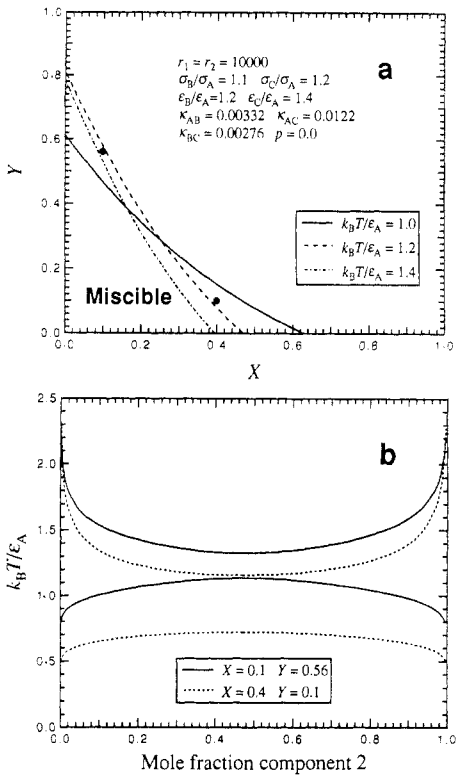

Figure 6. (a) Temperature dependence of the miscibility map for mixtures of random copolymers of type $(A_XB_{1-X})_{r_1}/(C_YB_{1-Y})_{r_2}$: $r_1 = r_2 = 10000$, $\sigma_B/\sigma_A = 1.1$, $\sigma_C/\sigma_A = 1.2$, $\epsilon_B/\epsilon_A = 1.2$, $\epsilon_C/\epsilon_A = 1.4$, $\kappa_{AB} = 0.00332$, $\kappa_{AC} = 0.0122$, $\kappa_{BC} = 0.00276$, $p = 0.0$. (b) Theoretical coexistence curves of copolymer mixtures corresponding to two pairs of copolymers denoted in (a).

copolymer in solvents or homopolymers varies with the copolymer composition. Figure 4a shows coexistence curves of two binary systems of type A_1/B_{500} and B_{20}/C_{20}. The segment fraction of component 2 is defined as $x_2r_2/(x_1r_1 + x_2r_2)$, where x_i and r_i are the mole fraction and the number of hard spheres per molecule of component i, respectively. For simplicity, let system A_1/C_{500} be identical to system A_1/B_{500}; these systems represent homopolymer–solvent solutions which exhibit both a LCST and an UCST. The system B_{20}/C_{20} is a homopolymer blend which is essentially immiscible in the temperature range shown in Figure 4a.

Copolymer solutions of type $A_1/C_YB_{1-Y})_{500}$ also exhibit both a LCST and an UCST. Figure 4b shows the copolymer composition dependence of reduced LCST and UCST, k_BT_c/ϵ_A; parameters are the same as those used in Figure 4a. The miscible temperature range increases as the copolymer composition rises; i.e., the solubility of homopolymer B_{500} is enhanced by making a copolymer with segments of type C which has unfavorable interaction with segments of type B.

Similar results can be obtained for the homopolymer/copolymer blend of type $A_{r_1}/(C_YB_{1-Y})_{r_2}$. Figure 5a shows the coexistence curves of two binary systems of type A_{10000}/B_{10000} and B_{1000}/C_{1000}. For simplicity, systems A_{10000}/B_{10000} and A_{10000}/C_{10000} are assumed to be identical; these systems represent homopolymer blends which exhibit both a LCST and an UCST. The system B_{1000}/C_{1000} is a homopolymer blend which is essentially immiscible. The homopolymer/copolymer blend of type $A_{10000}/(C_YB_{1-Y})_{10000}$ also exhibits both a LCST and an UCST. Figure 5b shows the copolymer composition dependence of LCST and UCST. The miscible temperature range increases as the copolymer composition rises.

The enhanced solubility of copolymer can be explained as follows. Since the parameters are chosen such that the interactions between segments B and C are unfavorable, the presence of segment C among segment B in copolymers gives interactions that are less favorable between the copolymers than those between homopolymers consisting of segment B only. Therefore, interactions between copolymer and solvent relative to those between copolymers become more favorable, resulting in increased solubility of copolymer in solvent A or homopolymer consisting of segments of type A. These results imply that a copolymer and a homopolymer can be miscible even though the corresponding three binary mixtures of homopolymers are immiscible.[17]

Figure 6a shows the miscibility map for mixtures of random copolymers of type $(A_XB_{1-X})_{r_1}/(C_YB_{1-Y})_{r_2}$ at three reduced temperatures, $\tilde{T}_A = k_BT/\epsilon_A$. A mixture of this type has a miscible region near the origin $X = Y = 0$. When $X = Y = 0$, components 1 and 2 are identical and there is complete miscibility. The theoretical coexistence curves of two pairs of copolymers—($X = 0.1$, $Y = 0.56$) and ($X = 0.4$, $Y = 0.1$)—are also shown in Figure 6b. While for small values of Y the miscible area monotonically decreases, for large values of Y the miscible area first increases and then decreases as $\tilde{T}_A$ rises from 1.0 to 1.4. This behavior occurs because immiscibility is caused by LCST behavior for small values of Y at $\tilde{T}_A$ above 1.0. On the other hand, immiscibility is caused by UCST behavior for large values of Y at $\tilde{T}_A = 1.0$. If a pair of copolymers are immiscible due to UCST behavior, the mixture becomes miscible as the temperature starts to exceed the UCST of the mixture. As the temperature rises further, however, the mixture eventually becomes immiscible because of the

presence of a LCST at elevated temperature.

Comparison with Experiment. The equation-of-state parameters for copolymer mixtures are obtained as follows. Consider component 1, a copolymer of type $(A_XB_{1-X})_{r_1}$. We use the regressed parameters ϵ_A, σ_A, and r/M of homopolymer consisting of segment A reported in ref 4 as the characteristic parameters of segment A in copolymers; here M is the molecular weight. These parameters were obtained from pure-component pressure–volume–temperature data. When the copolymer composition in weight fraction and the number-average molecular weight are known, simple stoichiometry gives ω_A, the total mass of segment A per mole of copolymer; ω_A is then multiplied by r/M of homopolymer consisting of segment A to obtain the number of effective hard spheres of type A, $r_{1,A}$. A similar calculation is performed to obtain $r_{1,B}$, the number of effective hard spheres of type B.

When the copolymer composition in weight fraction and the molecular weight are not reported and the miscibility map at constant chain volume, v_1^*, is reported as a function of the volume fraction of segment A, $\phi_{1,A}$, we assume that these parameters are related to the equation-of-state parameters by

$$r_{1,A} = \frac{\phi_{1,A} v_1^*}{{}^1/_6 \pi \sigma_{1,A}^3} \tag{48}$$

A similar equation for $r_{1,B}$ is obtained by replacing subscript A by B in eq 48. The total number of effective hard spheres per molecule, r_1, is therefore given by $r_{1,A} + r_{1,B}$. The number fraction of segment A, X, is then computed as $X = r_{1,A}/r_1$. Equation 48 assumes that the calculated chain volume is equal to the hard-core volume of a hard-sphere chain and that the reported volume fraction of segment A is equal to the hard-core volume fraction of segment A in a hard-sphere chain.

The chain volume of a copolymer molecule of known molecular weight and copolymer composition in weight fraction is usually calculated by assuming an additivity of volumes of repeat units. The volumes of repeat units are taken to be those of corresponding comonomers or the volumes calculated from the measured densities of corresponding homopolymers. Since the experimentally determined volumes of repeat units include free volumes, eq 48 would overestimate the total number of effective hard spheres per molecule. This is not a serious problem, however, because miscibility maps of copolymer mixtures are not sensitive to the molecular weight of copolymers when the molecular weight is sufficiently high.

Depending on the volumes of repeat units used to compute the volume fractions of segments, the assumed equality of reported volume fractions of segments and hard-core volume fractions of segments in a hard-sphere chain could result in slightly inaccurate number fractions of segments in a hard-sphere chain. This assumption may result in slightly incorrect locations of calculated boundaries between the miscible and immiscible regions on miscibility maps. This discrepancy is also not serious, however, because the systems studied in this paper have relatively large miscible areas.

The main objective of comparison of theoretical miscibility maps with experiment is to show that the PHSC equation of state can explain immiscibilities caused by LCST behavior. The assumptions in eq 48 will not affect the theoretical predictions regarding the origin of immiscibilities in the mixture. When the theory is compared with experiment, however, it is desirable to calculate the number fraction of segments and the total number of effective hard spheres per molecule from the molecular weight and the copolymer composition in weight fraction.

Table 1. Characterization of Polymer Samples Used in Refs 18 and 19

sample desig	polymer type	styrene content (wt %)	mol wt (M_n)[a]	M_w/M_n[a]
PBD	polybutadiene	0	2350	1.13
PS1	polystyrene	100	1900	1.06
PS2	polystyrene	100	2220	1.08
PS3	polystyrene	100	3302	1.06
PS4	polystyrene	100	5200	1.10–1.14
R50/50	poly(styrene-*co*-butadiene) random copolymer	50	24000	1.00
R25/75	poly(styrene-*co*-butadiene) random copolymer	25	27000	1.07

[a] M_n = number-average molecular weight. M_w = weight-average molecular weight.

Table 2. PHSC Equation-of-State Parameters for Homopolymers[4]

polymer	r/M (mol/g)[a]	σ (Å)	ϵ/k_B (K)
cis-1,4-polybutadiene	0.01499	5.264	611.8
polystyrene	0.01117	5.534	724.7
poly(methyl methacrylate)	0.01432	4.850	655.9
poly(butyl methacrylate)	0.01899	4.550	510.8

[a] M = molecular weight.

In addition to the intersegmental parameter κ_{AB}, for the mixture of type $(A_XB_{1-X})_{r_1}/(A_YB_{1-Y})_{r_2}$ we introduce an additional adjustable intersegmental parameter ζ_{AB} such that

$$b_{ij,AB}^{1/3} = \frac{b_{i,A}^{1/3} + b_{j,B}^{1/3}}{2}(1 - \zeta_{AB}) \qquad (i,j = 1,2) \tag{49}$$

ζ_{AB} therefore relaxes the additivity of effective hard-sphere diameters of unlike segments. When the experimental coexistence curve is available, these parameters can be obtained from the critical point of homopolymer blends of type A_{r_1}/B_{r_2}.

Equation 49 is different from the combining rule used in ref 6. In the present paper we use eq 49 because, when the molecular-weight dependence of the critical temperature is compared with experiment, the combining rule given by eq 49 gives better agreement with experiment.

We first compare theory with experiment for systems containing butadiene and styrene segments. Several experimental cloud-point curves of these systems are reported by Roe and Zin[18] and Park and Roe.[19] Tables 1 and 2 give characterizations of the polymer samples used by these authors and the PHSC equation-of-state parameters of polystyrene and polybutadiene homopolymers.

Intersegmental parameters, κ_{AB} and ζ_{AB}, are obtained from the observed critical point of the (PBD–PS1) system.[19] The experimental critical point, however, is very difficult to determine. In this paper we obtain two sets of intersegmental parameters by assuming two different critical points. We show calculated results based on each set.

Figure 7a shows a comparison of theoretical coexistence curves with experiment for the (PBD–PS1) system.[19] Two sets of intersegmental parameters obtained from the critical point are given in Table 3. Parameter sets 1 and 2 are obtained by assuming that the critical polystyrene weight fractions are 0.59 and 0.585, respectively. In both calculations the critical temperature is assumed to be 122 °C. The theoretical curve with parameter set 2 is slightly wider than that with parameter set 2. The width of the

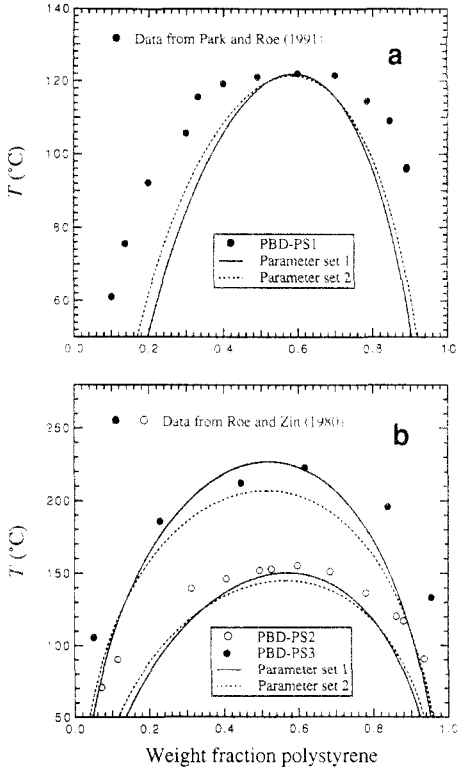

Figure 7. Comparison of theoretical existence curves with experiment for polybutadiene/polystyrene mixtures: (a) (PBD–PS1) system; (b) (PBD–PS2) and (PBD–PS3) systems. The curves in (b) are predictions. Characterizations of polymer samples are given in Table 1. Equation-of-state parameters and intersegmental parameters are given in Tables 2 and 3, respectively.

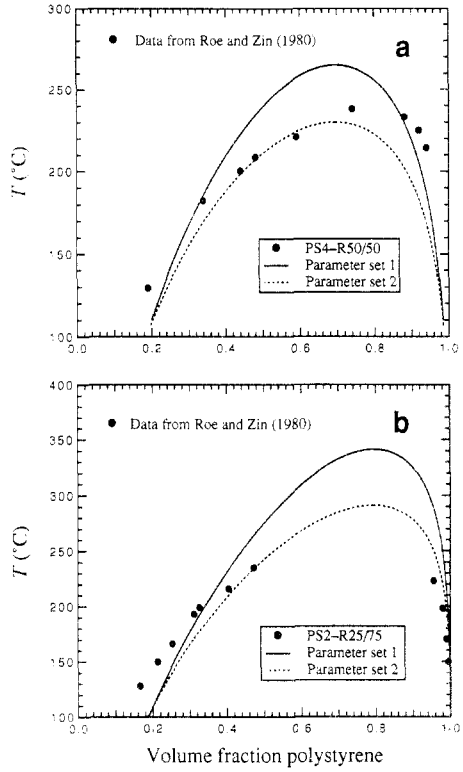

Figure 8. Comparison of predicted coexistence curves with experiment for polystyrene/poly(styrene-*co*-butadiene) mixtures: (a) (PS4–R50/50) system; (b) (PS2–R25/75) system. Characterizations of polymer samples are given in Table 1. Equation-of-state parameters and intersegmental parameters are given in Tables 2 and 3, respectively.

Table 3. Intersegmental Parameters

binary pair	κ_{AB}	ζ_{AB}
butadiene–styrene (parameter set 1)	0.00412	0.00026
butadiene–styrene (parameter set 2)	0.00544	0.00117
butyl methacrylate–methyl methacrylate	−0.00158	−0.001
styrene–butyl methacrylate	0.01085	−0.002

coexistence curve, however, is narrower than that from experiment. Next, we predict the coexistence curves of other systems containing styrene and butadiene segments, including random copolymers, using the binary parameters obtained above.

Figure 7b compares predicted coexistence curves with experiment for the systems (PBD–PS2) and (PBD–PS3).[18] The critical temperatures predicted by the theory with parameter set 1 agree well with experiment. The critical temperatures predicted by the theory with parameter set 2, however, are slightly lower than the experimental critical temperatures.

Parts a and b of Figure 8 compare predicted coexistence curves with experiment for the systems (PS4–R50/50) and (PS2–R25/75), respectively.[18] The predicted coexistence curves are plotted against the hard-core volume fraction of polystyrene. In these systems one component is a random copolymer. In both systems the theoretical coexistence curves with parameter set 2 give slightly better agreement with experiment than those with parameter set 1.

The results shown in Figures 7 and 8 indicate that predicted critical temperatures are sensitive to the choice of the critical point of a mixture where intersegmental parameters κ_{AB} and ζ_{AB} are to be obtained. It is therefore necessary to obtain these parameters such that the molecular-weight dependence of critical temperatures is correctly predicted by the model.

Figure 9 compares theoretical miscibility maps at two temperatures with experimental data by Braun *et al.*[20] for a mixture of type $(A_XB_{1-X})_{r_1}/(A_YB_{1-Y})_{r_2}$ containing poly(butyl methacrylate-*co*-methyl methacrylate) random copolymers. Braun *et al.* carried out experiments at a constant chain volume v_1^* of 130 nm^3. Details of characterization of the copolymer samples, however, are not reported. We assume that the chain volume is equal to the hard-core volume of hard-sphere chains, that is,

$$v_1^* = r_{1,A}\frac{\pi\sigma_{1,A}^3}{6} + r_{1,B}\frac{\pi\sigma_{1,B}^3}{6} \tag{50}$$

where subscripts A and B denote the butyl methacrylate and methyl methacrylate segments, respectively. For a given volume fraction of segment A, $\phi_{1,A}$, the number of segments A per molecule, $r_{1,A}$, is calculated by eq 48. Equation 50 then gives the number of segments of type B per molecule, $r_{1,B}$.

The intersegmental parameters were obtained as follows. We first assume a reasonable value of ζ_{AB} (for example, $\zeta_{AB} = 0.0$) and then compute κ_{AB} assuming that at 25 °C the boundary between miscible and immiscible regions at $\phi_{1,A} = 1.0$ lies at $\phi_{2,A} = 0.74$. The best fit was obtained with $\zeta_{AB} = -0.001$. Table 3 gives the values of the intersegmental parameters. The theory predicts that the immiscibility in this system is caused by LCST behavior. Also shown in Figure 9 is the miscibility map at 180 °C. The theoretical miscibility map was computed using parameters obtained at 25 °C. Although the choice of ζ_{AB} is somewhat arbitrary, the agreement of the predicted miscibility map with experiment at 180 °C is good.

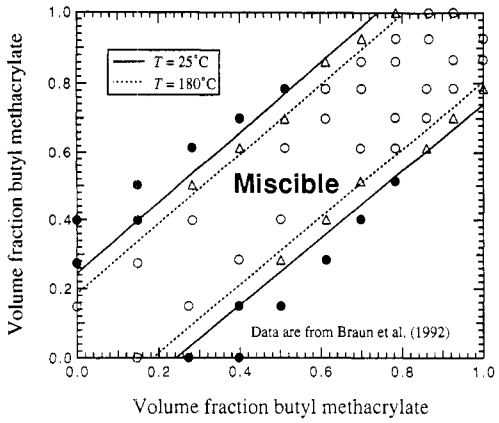

Figure 9. Comparison of theoretical miscibility maps with experiment for a mixture of type $(A_XB_{1-X})_{r_1}/(A_YB_{1-Y})_{r_2}$ containing poly(butyl methacrylate-*co*-methyl methacrylate) random copolymers. The theory predicts that immiscibility is caused by LCST behavior. Data are from Braun *et al.*:[20] (○) miscible at 25 and 180 °C; (△) miscible at 25 °C but immiscible at 180 °C; (●) immiscible at 25 and 180 °C. Equation-of-state parameters and intersegmental parameters are given in Tables 2 and 3, respectively.

Classical incompressible lattice theory such as the Flory–Huggins theory[21] predicts that for mixtures of type $(A_XB_{1-X})_{r_1}/(A_YB_{1-Y})_{r_2}$ a pair of copolymers is miscible if the copolymer composition difference $|X - Y|$ is smaller than a critical value $|X - Y|_c$ which is independent of the copolymer compositions. The miscibility of the system shown in Figure 9 follows the prediction of the Flory–Huggins theory. The temperature dependence of miscibility maps of this mixture, however, cannot be explained by the incompressible Flory–Huggins theory, which can predict an UCST only. The incompressible Flory–Huggins theory predicts that the miscible area increases as the temperature rises. Equation-of-state theory is necessary to explain the immiscibility caused by LCST behavior.[22-25]

Figure 10 compares theoretical miscibility maps with experiment obtained by Braun *et al.*[20] for mixtures of type $(A_XB_{1-X})_{r_1}/(A_YB_{1-Y})_{r_2}$ containing poly(styrene-*co*-butyl methacrylate) random copolymers. The average chain volume v_1^* is reported to be 230 nm^3. We first assume a value of ζ_{AB} and then solve for κ_{AB} assuming that at 25 °C the boundary between miscible and immiscible regions at $\phi_{1,A} = 1.0$ lies at $\phi_{2,A} = 0.70$; here subscripts A and B denote styrene and butyl methacrylate segments, respectively. The best fit was obtained with $\zeta_{AB} = -0.002$. Table 3 gives intersegmental parameters. These parameters are used to predict the miscibility map at 180 °C. The theory predicts that immiscibility is caused by LCST behavior. The miscible area therefore decreases as the temperature rises.

In the system shown in Figure 10, the critical composition difference $|X - Y|_c$ strongly depends on the copolymer compositions. Although the theory can qualitatively describe the dependence of critical composition difference on copolymer compositions and temperature, agreement with experiment is not as good as that for the system shown in Figure 9. Better agreement would be obtained by considering the dyad interactions as proposed by Braun *et al.*[20] The effect of dyad interactions can be introduced into the equation of state by expanding the perturbation term by dyad fraction. In this model the interaction energy between segments A belonging to different AA dyads is assumed to be different from the interaction energy between segment A in an AA dyad and segment A of an AB dyad. The physical interpretation of this assumption is that the presence of segment B in AB dyads produces a screening effect on the interaction of segment A of AB dyads with segment A of AA dyads.

Conclusions

A perturbed hard-sphere-chain (PHSC) equation of state for copolymer systems is presented. PHSC uses the modified Chiew equation of state for athermal mixtures of heteronuclear hard-sphere chains by Song *et al.* and a van der Waals perturbation. The Song–Mason method relates equation-of-state parameters to the segment–segment intermolecular potential. The PHSC equation of state can explain immiscibility due to lower critical solution temperature behavior in binary polymer blends containing copolymers. Theoretical coexistence curves and miscibility maps are compared with experiment for binary systems containing two kinds of segments. Theoretical miscibility maps are in good agreement with experiment for the system containing poly(butyl methacrylate-*co*-methyl methacrylate) random copolymers. The theory also gives semiquantitative agreement with experiment for systems containing poly(styrene-*co*-butadiene) and poly(styrene-*co*-butyl methacrylate) random copolymers.

Acknowledgment. This work was supported by the Director, Office of Energy Research, Office of Basic Energy Sciences, Chemical Sciences Division of the U.S. Department of Energy under Contract No. DE-AC03-76SF0098. Additional funding was provided by E. I. du Pont de Nemours & Co. (Philadelphia, PA) and Koninklijke Shell (Amsterdam, The Netherlands). The authors thank S. M. Lambert for useful discussions concerning the pure-component parameters of homopolymers.

Appendix A. Chemical Potential

Consider mixtures of heteronuclear hard-sphere chains. The chemical potential of component n, μ_n, is given by

$$\frac{\mu_n}{k_BT} = \frac{\mu_n^\circ}{k_BT} + \int_0^\rho \left[\frac{V}{k_BT}\left(\frac{\partial p}{\partial N_n}\right)_{T,V,N} - 1\right]\frac{d\rho}{\rho} +$$

$$\ln(x_n\rho k_BT) + 1 = \frac{\mu_n^\circ}{k_BT} + 2\rho\sum_{i=1}^{m} x_i\left[\sum_{k=1}^{r_i}\sum_{l=1}^{r_n} b_{in,kl}W_{in,kl}\right] +$$

$$\frac{\rho^2}{4}\sum_{i=1}^{m}\sum_{j=1}^{m} x_ix_j\left\{\sum_{k=1}^{r_i}\sum_{l=1}^{r_j} b_{ij,kl}\left[(\sum_{k=1}^{r_n} b_{n,k})X_{ij,kl} + (\sum_{k=1}^{r_n} b_{n,k}^{2/3})\left(\frac{b_{i,k}b_{j,l}}{b_{ij,kl}}\right)Y_{ij,kl}\right]\right\} - \sum_{k=1}^{r_n-1} Q_{nn,k,k+1} -$$

$$\frac{\rho}{4}\sum_{i=1}^{m} x_i\sum_{k=1}^{r_i-1}\left[(\sum_{k=1}^{r_n} b_{n,k})g_{ii,k,k+1} + (\sum_{k=1}^{r_n} b_{n,k}^{2/3})\left(\frac{b_{i,k}b_{i,k+1}}{b_{ii,k,k+1}}\right)H_{ii,k,k+1}\right] -$$

$$\frac{2\rho}{k_BT}\sum_{i=1}^{m} x_i\left[\sum_{k=1}^{r_i}\sum_{l=1}^{r_n} a_{in,kl}\right] + \ln(x_n\rho k_BT) + 1 \quad (A.1)$$

where μ_n° is the chemical potential per molecule of component n in the reference state, $W_{in,kl}$ and $Q_{nn,k,k+1}$ are given by eqs 35 and 36, respectively, and

$$X_{ij,kl} = \left(\frac{1}{\rho^2}\right)\int_0^\rho\left(\frac{\partial g_{ij,kl}}{\partial\eta}\right)\rho\, d\rho \quad (A.2)$$

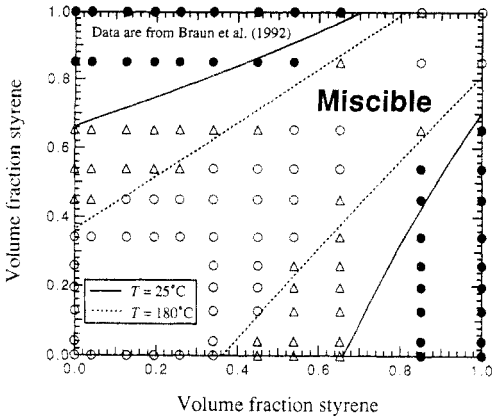

Figure 10. Comparison of theoretical miscibility maps with experiment for mixtures of type $(A_XB_{1-X})_{r_1}/(A_YB_{1-Y})_{r_2}$ containing poly(styrene-*co*-butyl methacrylate) random copolymers. The theory predicts that immiscibility is caused by LCST behavior. Data are from Braun *et al.*:[20] (○) miscible at 25 and 180 °C; (△) miscible at 25 °C but immiscible at 180 °C; (●) immiscible at 25 and 180 °C. Equation-of-state parameters and intersegmental parameters are given in Tables 2 and 3, respectively.

$$Y_{ij,kl} = \left(\frac{1}{\rho^2}\right)\int_0^\rho \left(\frac{\partial g_{ij,kl}}{\partial \xi_{ij,kl}}\right)\rho \, d\rho \tag{A.3}$$

$$H_{ii,k,k+1} = \left(\frac{1}{\rho}\right)\int_0^\rho \left(\frac{\partial g_{ii,k,k+1}}{\partial \xi_{ii,k,k+1}}\right) d\rho \tag{A.4}$$

The reference state is taken to be the pure ideal gas at unit pressure and at the temperature of the mixture containing the same number of molecules as the total number of molecules in the mixture.

The chemical potentials are related to the Gibbs energy, G, by

$$G = \sum_{i=1}^{m} N_i \mu_i \tag{A.5}$$

where

$$\frac{G}{Nk_BT} = \frac{A}{Nk_BT} + \frac{p}{\rho k_BT} \tag{A.6}$$

where A is the Helmholtz energy given by eq 34.

References and Notes

(1) Wohlfarth, C. *Makromol. Chem., Theory Simul.* **1993**, *2*, 605.
(2) Guggenheim, E. A. *Mixtures*; Clarendon Press: Oxford, 1952.
(3) Song, Y.; Lambert, S. M.; Prausnitz, J. M. *Macromolecules* **1994**, *27*, 441.
(4) Song, Y.; Lambert, S. M.; Prausnitz, J. M. *Ind. Eng. Chem. Res.* **1994**, *33*, 1047.
(5) Song, Y.; Lambert, S. M.; Prausnitz, J. M. *Chem. Eng. Sci.*, in press.
(6) Song, Y.; Lambert, S. M.; Prausnitz, J. M. Paper presented at the AIChE meeting in St. Louis, November 1993.
(7) Chiew, Y. C. *Mol. Phys.* **1990**, *70*, 129.
(8) Song, Y.; Mason, E. A. *J. Chem. Phys.* **1989**, *91*, 7840.
(9) Sanchez, I. C.; Lacombe, R. H. *J. Phys. Chem.* **1976**, *80*, 2352.
(10) Sanchez, I. C.; Lacombe, R. H. *Macromolecules* **1978**, *11*, 1145.
(11) Chapman, W. G.; Gubbins, K. E.; Jackson, G.; Radosz, M. *Ind. Eng. Chem. Res.* **1990**, *29*, 1709.
(12) Huang, S. H.; Radosz, M. *Ind. Eng. Chem. Res.* **1990**, *29*, 2284.
(13) Song, Y. Ph.D. Dissertation, Brown University, 1991.
(14) Balazs, A. C.; DeMeuse, M. T. *Macromolecules* **1989**, *22*, 4260.
(15) Prausnitz, J. M.; Lichtenthaler, R. N.; de Azevedo, E. G. *Molecular Thermodynamics of Fluid-Phase Equilibria*, 2nd ed.; Prentice-Hall Inc.: Englewood Cliffs, NJ, 1986; Chapter 3.
(16) McMaster, L. P. *Macromolecules* **1973**, *6*, 760.
(17) Paul, D. R.; Barlow, J. W. *Polymer* **1984**, *25*, 487.
(18) Roe, R. J.; Zin, W. C. *Macromolecules* **1980**, *13*, 1221.
(19) Park, D. W.; Roe, R. J. *Macromolecules* **1991**, *24*, 5324.
(20) Braun, D.; Yu, D.; Kohl, P. R.; Gao, X.; Andradi, L. N.; Manger, E.; Hellmann, G. P. *J. Polym. Sci., Polym. Phys. Ed.* **1992**, *30*, 577.
(21) Hino, T.; Lambert, S. M.; Soane, D. S.; Prausnitz, J. M. *Polymer* **1993**, *34*, 4756.
(22) Shiomi, T.; Ishimatsu, H.; Eguchi, T.; Imai, K. *Macromolecules* **1990**, *23*, 4970.
(23) Shiomi, T.; Ishimatsu, H.; Eguchi, T.; Imai, K. *Macromolecules* **1990**, *23*, 4978.
(24) Kim, C. K.; Paul, D. R. *Polymer* **1992**, *33*, 1630.
(25) Kim, C. K.; Paul, D. R. *Polymer* **1992**, *33*, 2089.